Geomorphology 122 (2010) 205–210

Contents lists available at ScienceDirect

Geomorphology

journal homepage: www.elsevier.com/locate/geomorph

Geomorphic and climatic controls on chemical weathering in the High Himalayas of Nepal

Emmanuel J. Gabet [a,*], Domenik Wolff-Boenisch [b], Heiko Langner [c], Douglas W. Burbank [d], Jaakko Putkonen [e]

[a] Department of Geology, San Jose State University, San Jose, CA 95192, USA
[b] Institute of Earth Sciences, University of Iceland, 101 Reykjavik, Iceland
[c] Department of Geosciences, University of Montana, Missoula, MT 59802, USA
[d] Department of Earth Sciences, University of California, Santa Barbara, CA 93106, USA
[e] Department of Geology and Geological Engineering, University of North Dakota, Grand Forks, ND 58202, USA

ARTICLE INFO

Article history:
Received 4 April 2010
Received in revised form 29 June 2010
Accepted 30 June 2010
Available online 7 July 2010

Keywords:
Erosion
Chemical weathering
Himalayas
Glaciers
Marsyandi

ABSTRACT

The hypothesis that CO_2 consumption by chemical weathering is enhanced by the exposure of fresh minerals provides a mechanism linking tectonic, geomorphic, and atmospheric processes. We present data from the High Himalayas of Nepal indicating a positive linear relationship between cation weathering rate and suspended sediment yield. Because of a steep precipitation gradient across the field area, the weathering rates are normalized according to runoff to isolate erosion as the controlling factor. Adjusted for runoff, increases in weathering rates do not keep pace with increasing erosion rates where suspended sediment yields >2000 t/km^2/y. This result supports studies that predict a nonlinear relationship between denudation and weathering in rapidly eroding landscapes. In addition, we document a decoupling of the weathering of Si and silicate cations from a glacierized watershed. The proportions of silicate-derived Na and K are high relative to Si during the warm summer months and then drop when subfreezing temperatures arrive in the fall. We propose that, during the summer, glacial abrasion creates fresh mineral surfaces that favor the release of cations, and abundant meltwater flushes these weathering products from the subglacial bed. As temperatures fall below freezing and the production of meltwater slows dramatically, river discharge becomes dominated by groundwater bearing the chemical signature of more congruent weathering reactions.

1. Introduction

In 1952, Urey (1952) linked climatic and geochemical processes by proposing that the weathering of Ca- and Mg-bearing silicate minerals sequesters atmospheric CO_2 through the ultimate precipitation of calcite and dolomite. Since then, a concerted effort has been made to understand the fundamental controls on chemical weathering (e.g., Berner, 1978; White and Blum, 1995; Kump et al., 2000; West et al., 2005). These investigations have been stimulated by conceptual and numerical models that propose links and feedbacks between atmospheric processes, weathering, tectonic processes, and erosion (e.g., Berner et al., 1983; Raymo et al., 1988; Raymo and Ruddiman, 1992; Berner, 1994).

Climate, as represented by temperature and precipitation, has been identified as a critical factor influencing silicate weathering rates. The role of temperature is particularly interesting because of the potential negative feedback between climate and silicate weathering rates. Increases in atmospheric CO_2 would raise global temperatures through greenhouse effects; the increase in temperature, in turn, should enhance silicate weathering rates and lead to a decrease in atmospheric CO_2, thus bringing temperatures back down (Walker et al., 1981; Berner et al., 1983). In support of this hypothesis, White and colleagues (White and Blum, 1995; White et al., 1999) concluded from the analysis of field data that the weathering of Si and silicate-derived Na are primarily controlled by climatic factors. Similarly, others have determined that chemical denudation rates were correlated with runoff, a proxy for precipitation (Dunne, 1978; Kump et al., 2000; West et al., 2002; France-Lanord et al., 2003).

In contrast, other studies have concluded that the exposure of fresh mineral surfaces by erosion is the most important factor determining rates of chemical weathering (Stallard and Edmond, 1983; Edmond et al., 1996; Huh and Edmond, 1999; Oliva et al., 2003). Indeed, Riebe et al. (2001) and Millot et al. (2002) found that chemical denudation was strongly correlated to erosion rate. The potential influence of erosion on chemical weathering rates is intriguing because it provides a link between tectonic and atmospheric processes. Of course, both climate and erosion likely have important influences on chemical weathering (Gaillardet et al., 1999; France-Lanord et al., 2003), and statistical models have been employed to

* Corresponding author. Tel.: +1 408 924 5035; fax: +1 408 924 5050.
E-mail address: manny.gabet@sjsu.edu (E.J. Gabet).

0169-555X/$ – see front matter © 2010 Elsevier B.V. All rights reserved.
doi:10.1016/j.geomorph.2010.06.016

disentangle the relative contributions of temperature, precipitation, and physical denudation (Riebe et al., 2004; West et al., 2005).

Although evidence indicates that chemical weathering in the Himalayas was insufficient to have triggered global cooling in the Cenozoic (e.g., Galy and France-Lanord, 1999; France-Lanord et al., 2003; Wolff-Boenisch et al., 2009), as originally proposed by Raymo and Ruddiman (1992), the high rates of erosion and the steep gradients in temperature and precipitation make it a useful region for studying the controls on chemical weathering rates. In this contribution, we compare solute and sediment yield data from the Annapurna region of central Nepal, a zone that spans the breadth of the High Himalayas and reaches into the Tibetan Plateau (Fig. 1). Whereas others (e.g., France-Lanord et al., 2003) have previously investigated the general relationship between erosion and weathering in Nepal, the present study benefited from an intensive river monitoring program and a vast network of meteorological stations, thus offering an unprecedented level of spatial and temporal detail in the data collected.

2. Methods

2.1. Field site

In 2000–2001, 10 river monitoring stations were established along the Marsyandi River and selected tributaries (Fig. 1; Table 1). This area is one of the wettest in the High Himalayas (Bookhagen and Burbank, 2006) and has a strong precipitation gradient: runoff increases twenty-fold along a 40-km transect. Air temperature was measured at 17 meteorological stations deployed throughout the field area at elevations ranging from 1500 to 4400 m (Putkonen, 2004). The data from the meteorological stations were used to derive a lapse rate of 5 °C/km, thus allowing us to estimate temperatures in areas beyond the reach of the network.

The region is sparsely populated and only a small proportion ($\ll$5%) of the area is cultivated, inhabited, or logged, thus minimizing the effects of human land use impacts. Some of the watersheds in the study area are glacierized, with the area covered by glaciers ranging from 0 to 21% (Table 1); the dominant erosional process on the unglacierized slopes is landsliding (Gabet et al., 2004; Gabet et al., 2008). Bedrock in the study area includes sedimentary units of the Tethyan sequence, gneisses of the Greater Himalayan sequence, and schists and limestones of the Lesser Himalayan sequence (Colchen et al., 1986; Searle and Godin, 2003) (Fig. 1).

2.2. River sampling

In 2000–2002, channel cross sections at each station were surveyed, flow velocities were measured, and stage poles were installed to develop stage–discharge rating curves (Gabet et al., 2008). During the monsoon seasons (June–October), stage was recorded and three suspended sediment samples were taken twice daily at each station; outside of the monsoon seasons, stage was recorded less frequently. The suspended sediment samples from each sampling interval were filtered (25 μm mesh), dried, weighed, and averaged. The average suspended sediment concentration was multiplied by the discharge, calibrated with data from the Tropical Rainfall Measuring Mission (Bookhagen and Burbank, 2006; Gabet et al., 2008), to calculate a suspended sediment load; sediment loads were integrated

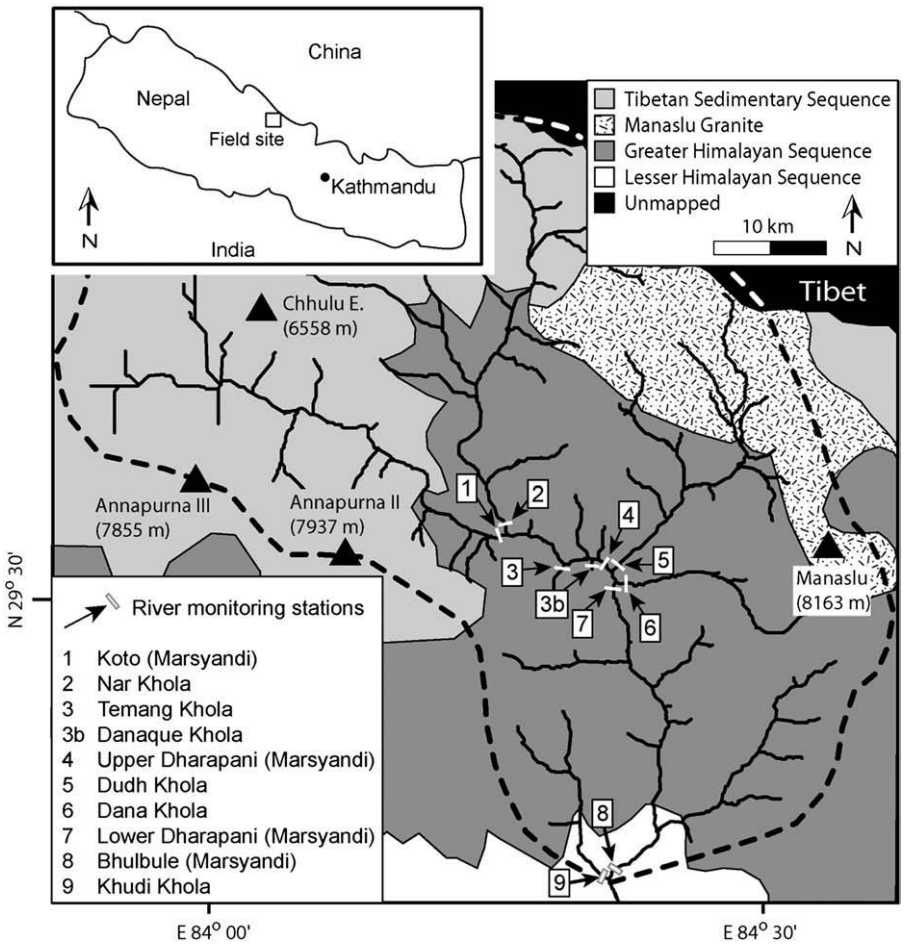

Fig. 1. Study area with the locations of river monitoring stations. Site names shown in legend. Dashed line is watershed boundary. Lithological map modified from Searle and Godin (2003).

Table 1
Watershed data.

Station	Basin #	Lithology[a]	Mean annual air temp. °C	Runoff[b] m/y	Total area km^2	Glacial cover %	Average elevation m	2000–2002 suspended sediment flux t/km^2/y	2002 sil. cation weath. rate[b] kmol/km^2/y
Koto	1	TSS	3	0.76	812	12	4794	1710	134.8
Nar	2	TSS	1	0.15	1052	10	5174	265	21.7
Temang[c]	*3*	*GHS*	*7*	*1.62*	*21*	*0*	*4087*	*186*	*117.9*
Danaque[c]	*3b*	*GHS*	*11*	*1.17*	*7*	*0*	*3349*	*1543*	*88.3*
Upper Dharapani	4	GHS	3	0.56	1946	11	4918	740	64.9
Dudh	5	GHS*	4	0.72	491	15	4694	435	30.3
Dana	6	GHS	3	1.09	156	21	4851	350	40.9
Lower Dharapani	7	GHS	3	0.44	2605	12	4870	688[d]	33.3
Bhulbule	8	LHS	5	0.76	3217	10	4522	914	69.0
Khudi	9	LHS	15	3.54	152	0	2566	3413	384.5

[a] TSS = Tibetan Sedimentary sequence; GHS$^{(*)}$ = Greater Himalayan sequence (*includes the Manaslu Granite); LHS = Lesser Himalayan sequence.
[b] Wolff-Boenisch et al. (2009).
[c] Italicized data not included in analyses (see Methods).
[d] Adjusted value (see text). Original value = 930.

throughout the monitoring season to produce an annual suspended sediment yield. Bedload yields could not be measured directly, and thus, suspended sediment yields are assumed to be approximately proportional to the total physical denudation rate. Bedload has been estimated to account for ~33% of the total load (Pratt-Sitaula et al., 2007; Gabet et al., 2008).

During the 2002 monsoon season, weekly water samples were collected, filtered, split, and one aliquot was preserved with nitric acid to pH~1. The solute data and a full description of the chemical analyses are presented in Wolff-Boenisch et al. (2009). Briefly, cation concentrations were determined through inductively-coupled plasma optical emission spectrometry, anion concentrations were measured through ion chromatography, and bicarbonate concentrations were determined through titration. Meteoric corrections were made with rainwater samples and hydrothermal inputs were accounted for with data from Tipper et al. (2006). The major cations were assigned to silicate sources according to Galy and France-Lanord (1999). Finally, silicate weathering rates were normalized according to the map area of silicate lithologies (Wolff-Boenisch et al., 2009).

Of the 10 monitored watersheds, two are significantly smaller than the rest (Danaque and Temang; Table 1). Given the short monitoring period, random landslides with unknown recurrence intervals can strongly influence calculations of the average annual suspended sediment yields from these small watersheds; thus, the data from these catchments are not included in the analyses. Whereas data from only eight stations may seem to offer limited insight, the twice-daily suspended sediment flux measurements and the weekly solute flux measurements provide an unprecedented sampling frequency for these processes in the High Himalayas. The accuracy and internal consistency of the data from this monitoring program were analyzed in Gabet et al. (2008) and found to be satisfactory. Note also that Gabet et al. (2008) calculated erosion rates for the region with records that spanned from 2000 to 2004. Here, we examine suspended sediment yields determined from records up to 2002 to match the solute data collected contemporaneously in 2002. Finally, although the watersheds were only intensively monitored during the monsoon, the discharges of water, sediment, and solutes during this period accounts for the majority of the annual totals from the high monsoonal flows (Tipper et al., 2006).

3. Results

A robust linear relationship emerges between the weathering rate of cations derived from silicate rocks and the suspended sediment flux (Fig. 2). The linearity of the relationship, however, is surprising when compared to results from others. The data presented in studies from diverse locations (Gaillardet et al., 1999; Riebe et al., 2001; Millot et al., 2002; Riebe et al., 2004; West et al., 2005; Hren et al., 2007) indicate that the dependency of chemical weathering (W) on erosion (E) can be represented as: $W \propto E^{\lambda}$, where λ is a dimensionless constant with a value depending on the weathering regime (Gabet and Mudd, 2009). In slowly eroding landscapes, chemical weathering is limited by the supply of fresh minerals and λ is close to unity (Riebe et al., 2004; Waldbauer and Chamberlain, 2005; West et al., 2005; Hren et al., 2007; Gabet and Mudd, 2009). As erosion rates increase, however, weathering becomes limited by the kinetics of the chemical reactions, and the value of λ falls below 1 such that further increases in erosion will not yield equivalent increases in chemical weathering (Millot et al., 2002; Waldbauer and Chamberlain, 2005; Gabet, 2007; Gabet and Mudd, 2009). For example, West et al. (2005) determined that, in kinetically limited situations, chemical weathering rates scale with approximately the square root of erosion rate; a similar value was found by Gabet (2007) in a theoretical study of landslide-dominated landscapes.

Wolff-Boenisch et al. (2009) concluded that chemical weathering in our study region was kinetically limited. In addition, a compilation from West et al. (2005) suggests that chemical weathering is kinetically limited where denudation rates are >50 t/km^2/y; the slowest eroding basin included in our analyses has a suspended sediment flux of 265 t/km^2/y (representing only a fraction of its total erosion rate). Therefore, a nonlinear relationship (with $\lambda<1$) between silicate cation weathering rate and suspended sediment flux would be expected. The role of rainfall in flushing soil pores and preventing the build-up of high solute concentrations that could inhibit dissolution is a likely explanation for the anomalous linear relationship (Kump et al., 2000). The watershed with the highest weathering rate (Khudi) is also the wettest, with an average annual runoff that is 5–20 times

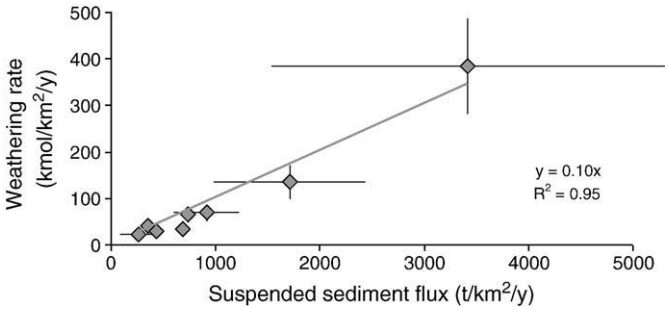

Fig. 2. Linear relationship between the weathering rate of silicate cations and suspended sediment flux, a proxy for erosion rate. X-axis error bars represent 1σ; y-axis error bars represent 27% uncertainty in weathering rates (Wolff-Boenisch et al., 2009).

higher than the others (Table 1). Although the Khudi catchment is also warmer than the others, diffusive proton–cation exchanges are less sensitive to temperature than the hydrolysis of Si–O bonds (Lasaga, 1998) and, thus, precipitation likely exerts a greater influence on cation weathering rates. Indeed, Dunne (1978) documented a strong relationship between runoff and chemical weathering and others have found that, of the two climatic parameters, precipitation has the strongest effect (France-Lanord et al., 2003; West et al., 2005). Finally, the air temperatures recorded by our meteorological stations likely are not representative of the temperatures at the glacial beds where some fraction of the glacierized watersheds' chemical weathering was taking place. Thus, to isolate the role of erosion in controlling chemical weathering, the measured cation weathering rates are normalized according to runoff (Table 1). Adapting West et al.'s (2005) approach, normalized weathering rates, W^*, are calculated for each watershed with

$$W^* = W\left(1 + \frac{\delta R}{R_0}\right)^{-\beta} \quad (1)$$

where W is the measured cation weathering rate, R_0 is the logarithmic mean of annual runoff from all the stations, δR is the difference between each watershed's annual runoff and R_0 (i.e., $R - R_0$), and β is a fitted parameter found by West et al. to have a value of 0.73 ± 0.20. Although Eq. (1) does not explicitly adjust for the effect of temperature, rainfall and temperature are highly correlated in the study area ($r = 0.98$; Pearson correlation coefficient), and thus the weathering rates are, to some extent, implicitly normalized for temperature.

Accounting for the influence of precipitation bends the linear relationship between weathering and erosion into one that is nonlinear, with the nonlinearity becoming apparent where erosion rates >2000 t/km^2/y (Fig. 3). These results support studies that have demonstrated that weathering rates initially increase linearly with erosion in slowly denuding landscapes but, as erosion rates reach ~ 10^3 t/km^2/y, increases in chemical weathering are unable to keep pace (West et al., 2005; Gabet and Mudd, 2009).

4. Discussion

4.1. Erosion and chemical weathering

The Himalayas were identified by Raymo and Ruddiman (1992) as a critical region where accelerated erosion would enhance chemical weathering rates. Our results suggest that, when erosion is isolated as the sole controlling factor, increases in chemical weathering in the Himalayas appear unable to keep pace with increases in denudation at the high end of erosion rates (Fig. 3). However, in reality, erosion does not operate in isolation, and in the Himalayas, it is strongly correlated with annual precipitation (Gabet et al., 2008). Therefore, to the extent that precipitation drives erosion rates and may even concentrate tectonic strain (Hodges et al., 2004), the linearity of the relationship between weathering and erosion (Fig. 2) suggests that increases in denudation may be associated with equivalent increases in cation weathering rates in the Himalayas. Uplift at the range front forces orographic precipitation that accelerates erosion rates and exposes fresher minerals to the humid environment. Indeed, the fastest eroding watershed, the Khudi, is the wettest, has the highest rates of chemical weathering, and appears to be in a zone of recent faulting (Wobus et al., 2003; Hodges et al., 2004). Nevertheless, although these processes are spatially related, the overlap is very localized; indeed, the Khudi watershed represents an area that is only a small fraction of the entire range. The effect of enhanced chemical weathering in the Khudi and similar Himalayan watersheds on global CO_2 levels is, thus, insignificant (Wolff-Boenisch et al., 2009).

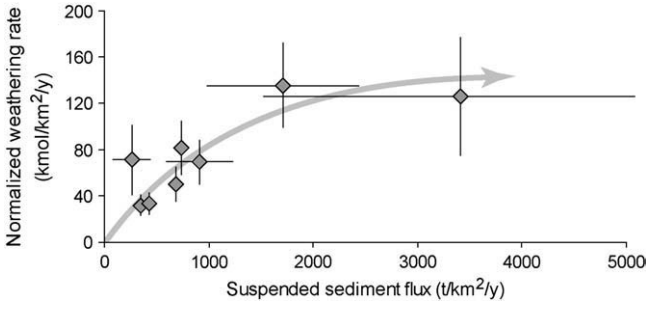

Fig. 3. Silicate cation weathering rate normalized by runoff vs. suspended sediment flux. Removing the influence of precipitation reveals that weathering rates increase nonlinearly with erosion. A regression equation is not fitted to the data because the nature of the relationship changes depending on the range of erosion rates (Gabet and Mudd, 2009). X-axis error bars represent 1σ; y-axis error bars represent 27% uncertainty in weathering rates and 27% uncertainty in B (from Eq. (1)) propagated through calculations of normalized weathering rates.

Finally, it is somewhat surprising that a clear relationship between erosion and weathering can be inferred from our data set. Most large-scale investigations of chemical weathering deliberately choose sites with similar bedrock, typically granite, to control for the effect of lithology on weathering rates (e.g., Riebe et al., 2004; West et al., 2005). In contrast, the watersheds in our study are underlain by a variety of silicate lithologies (e.g., granite, black shale, and gneiss) that may weather at different rates. Whereas the mosaic of different rock types might be expected to dilute the relationship between erosion and weathering, it does not appear to have an effect. It may be that, in mountainous landscapes, the dual influences of erosion and climate simply overwhelm any differences in weathering susceptibility arising from lithological differences. Another explanation may be that susceptibility to chemical weathering covaries with vulnerability to physical erosion for individual rock types: physically weak bedrock is likely to be broken up into small fragments with greater surface area vulnerable to chemical attack. In addition to the different lithologies, including watersheds eroded by different processes might also be expected to confound attempts to extract a relationship between denudation and erosion. In some watersheds, such as the Khudi, landslides are the dominant erosional process; in others, such as the Nar, glaciers are dominant; and in some, like the Dudh, both are important. Therefore, landslides and glaciers appear to be similarly efficient, within the measurement uncertainties, at pulverizing rock and creating fresh mineral surfaces.

4.2. Incongruent weathering in a glacierized watershed

Oliva et al. (2003) suggested that in rapidly eroding landscapes the weathering of Si and silicate cations are decoupled, with their rates responding to different forcing factors. Indeed, Wolff-Boenisch et al. (2009) demonstrated that the weathering of Si in the Annapurna region is dependent on temperature, whereas the results presented here suggest that the weathering of silicate cations is primarily dependent on erosion rate. Laboratory studies under relevant experimental conditions (circum-neutral pH, low temperature) have indicated that the weathering of fresh feldspar surfaces is characterized by an initial release of cations and then evolves towards stochiometric dissolution (Chou and Wollast, 1984; Muir et al., 1990; Hamilton et al., 2000). This progression has been attributed to the development of a silicon-rich layer on the surface of weathered minerals (Brantley, 2003; Fletcher et al., 2006). Supporting these laboratory studies, Anderson et al. (1997) and Hodson et al. (2000) noted low Si concentrations relative to cations in glacial runoff and suggested that subglacial grinding could stimulate the preferential release of cations. In our field area, the glacierized Nar watershed is well situated for exploring the role of erosion in incongruent weathering because glacial activity is seasonal: the glaciers are mainly

active during the summer and are relatively quiescent the rest of the year (Gabet et al., 2008). In addition, although only 10% of the Nar catchment is glacierized, its glaciers are the dominant source of runoff, sediment and, presumably, solutes because of its high altitude and relative aridity (Gabet et al., 2008). Other watersheds, such as the Dana, have a higher fraction of glacierized area but they also have greater rainfall, and thus, a variety of sources supply solutes to the runoff in unknown proportions.

Similar to Hodson et al. (2000), we use the molar ratio $([K_s]+[Na_s])/[Si]$, where the subscript 's' refers to silicate sources, as a measure of incongruent weathering (i.e., the ratio increases as incongruent weathering becomes more important). The source of the potassium is assumed to be biotite, and albite is assumed to be supplying the sodium, although amphiboles may also contribute. The concentration of Si reflects the weathering of Si from all silicate rocks, and thus, the absolute values of $([K_s]+[Na_s])/[Si]$ are essentially meaningless; however, changes in this ratio through time may signal changes in the chemical weathering processes. Potassium and sodium are chosen because their sources are well constrained. Rainwater samples were used to adjust for meteoric contributions, and Na from salt deposits was accounted for with Cl concentrations, leaving silicates as the major source after corrections for hydrothermal inputs (Wolff-Boenisch et al., 2009). In contrast, Ca and Mg have important carbonate sources, and thus, some uncertainty exists in determining the fraction of each from silicate sources.

As the seasons change from summer to fall, and the air temperature at the snout of the glaciers approaches 0 °C, discharge from the Nar watershed quickly decreases (Fig. 4). A steep decline in discharge in early September when temperatures drop below 2 °C indicates the arrival of freezing temperatures higher up on the glaciers and the slowing of meltwater production. During this period of cooling temperatures, the $([K_s]+[Na_s])/[Si]$ ratio initially decreases with the waning discharge and then becomes approximately constant when the flow drops below 30 m^3/s (Fig. 4). Given that temperature along the subglacial beds should not vary dramatically, the decrease in the ratio is unlikely to be directly related to the change in the weather. We propose, instead, that the shift away from incongruent weathering towards more congruent weathering may be explained by the seasonality of meltwater production. During the summer, when the glaciers in the Nar catchment are the most active (Gabet et al., 2008), the production of fresh mineral surfaces by glacial abrasion enhances the weathering of cations and the abundant meltwater flushes the solutes from the pulverized subglacial sediment (Anderson, 2005). In September, the colder temperatures inhibit the creation of meltwater, and thus, the delivery of cation-rich runoff slows; indeed, as the flow from the Nar watershed declines by 60%, the $([K_s]+[Na_s])/[Si]$ ratio decreases by 40%, and the total cation yield decreases by 70%. Anderson et al. (1997) also noted the importance of meltwater in controlling chemical weathering rates from glacierized basins. With the loss of meltwater as a significant source of runoff, the relative contribution of groundwater to the flow in the Nar River becomes more significant. Because the groundwater has had longer contact times with 'older' mineral surfaces, the lower values of $([K_s]+[Na_s])/[Si]$ may reflect more congruent weathering. For comparison, the $([K_s]+[Na_s])/[Si]$ ratios in the non-glacierized watersheds, such as the Khudi catchment, do not suggest a shift to more congruent weathering as temperature and discharge declines (Fig. 5). In these landslide-dominated basins, runoff is generated from hillslopes throughout the catchment and it flows over mineral surfaces with a fuller distribution of ages (Gabet, 2007). Therefore, in contrast to the Nar watershed, the diffuse nature of runoff generation in the Khudi basin spatially integrates the range of mineral surface ages.

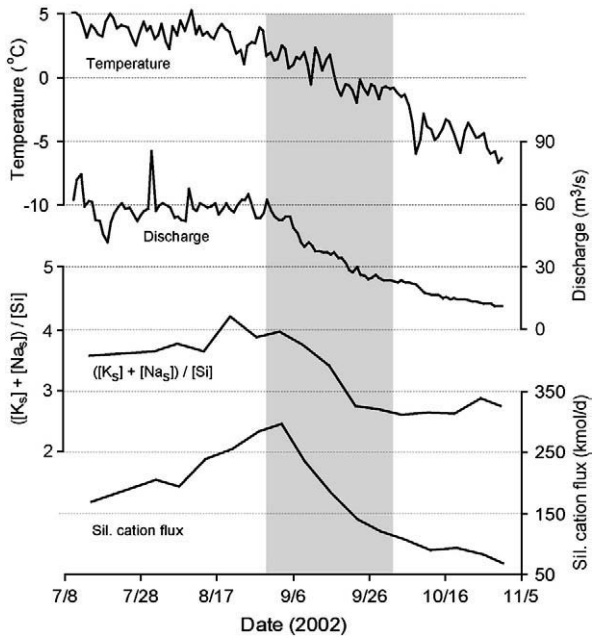

Fig. 4. Air temperature, river flow, cation:Si ratio, and total silicate cation flux from the Nar watershed. As temperatures at the snout of the glaciers dip below 2 °C in September (gray shading), discharge from glacial melt drops precipitously, weathering becomes more congruent (i.e., the cation:Si ratio decreases), and the total cation flux decreases.

5. Conclusion

Recently, great interest has been shown in identifying the controls on the weathering rate of silicate rocks. This interest has been motivated by attempts to link tectonic, geomorphic, and atmospheric processes. In this contribution, we present data from the High Himalayas of Nepal that document a strong linear relationship between silicate cation weathering rates and suspended sediment yields, a proxy for erosion rate. The linear relationship suggests that increases in weathering rate can match increases in erosion rate. The linearity of the relationship, however, disappears when the weathering rates are normalized according to runoff. Isolating erosion as the

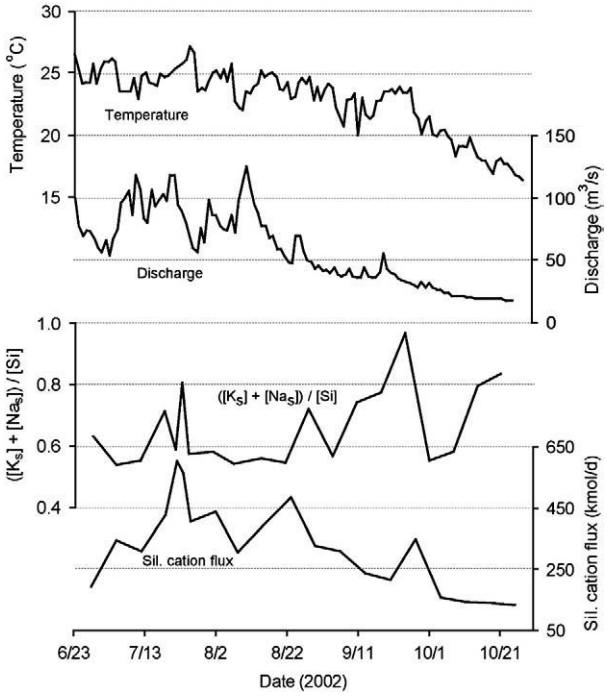

Fig. 5. Air temperature, river flow, cation:Si ratio, and total silicate cation flux from the Khudi watershed. In contrast to the Nar watershed, decreases in temperature, discharge, and total cation flux are not associated with a decrease in the cation:Si ratio. The $([K_s]+[Na_s])/[Si]$ ratio appears to rise slightly with the arrival of fall, perhaps reflecting the role of cooling temperatures in slowing Si dissolution rates.

sole factor in controlling weathering reveals that the increases in weathering rates begin to taper where physical denudation >2000 t/km^2/y. In addition, we present evidence suggesting that silicate cations are preferentially released from fresh mineral surfaces created by subglacial grinding. During the summer when glaciers are most active and abundant meltwater flushes solutes from the subglacial beds, silicate-derived Na and K have higher concentrations, relative to Si, than during the remainder of the year.

Acknowledgements

We thank A. Duvall, A. Sitaula, and A. Johnstone for field help; W. Amidon for map analysis; and S. Anderson, S. Brantley, A. White, S. Mudd, and E. Tipper for the discussions. J. West, K. Norton, and two anonymous reviewers are thanked for their attentive and insightful reviews. This research was funded by the National Science Foundation Continental Dynamics Program (EAR-9909647), by the National Aeronautics and Space Administration (NAGS-7781, NAGS-9039, NAGS-10520), and by the University of California, Riverside. Logistical support from Himalayan Experience and the Nepalese Department of Hydrology and Meteorology is gratefully acknowledged.

References

Anderson, S.P., 2005. Glaciers show direct linkage between erosion rate and chemical weathering fluxes. Geomorphology 67, 147–157.
Anderson, S.P., Drever, J.I., Humphrey, N.F., 1997. Chemical weathering in glacial environments. Geology 25 (5), 399–402.
Berner, R.A., 1978. Rate control of mineral dissolution under earth surface conditions. American Journal of Science 278, 1235–1252.
Berner, R.A., 1994. GEOCARB II: A revised model of atmospheric CO_2 over Phanerozoic time. American Journal of Science 294, 59–91.
Berner, R.A., Lasaga, A.C., Garrels, R.M., 1983. The carbonate-silicate geochemical cycle and its effect on atmospheric carbon-dioxide over the past 100 million years. American Journal of Science 283, 641–683.
Bookhagen, B., Burbank, D.W., 2006. Topography, relief, and TRMM-derived rainfall variations along the Himalaya. Geophysical Research Letters 33. doi:10.1029/2006GL026037.
Brantley, S.L., 2003. Reaction kinetics of primary rock-forming minerals under ambient conditions. In: Turekian, K.K., Holland, H.D. (Eds.), Treatise on Geochemistry. Pergamon Press, Oxford, Uk, pp. 73–117.
Chou, L., Wollast, R., 1984. Study of the weathering of albite at room temperature and pressure with a fluidized bed reactor. Geochimica et Cosmochimica Acta 48, 2205–2217.
Colchen, M., Le Fort, P., Pecher, A., 1986. Annapurna–Manaslu–Ganesh Himal. Centre National de la Recherche Scientifique, Paris.
Dunne, T., 1978. Rates of chemical denudation of silicate rocks in tropical catchments. Nature 274, 244–246.
Edmond, J.M., Palmer, M.R., Measures, C.I., Brown, E.T., Huh, Y., 1996. Fluvial geochemistry of the eastern slope of the northeastern Andes and its foredeep in the drainage of the Orinoco in Colombia and Venezuela. Geochimica et Cosmochimica Acta 60 (16), 2949–2976.
Fletcher, R.C., Buss, H.L., Brantley, S.L., 2006. A spheriodal weathering model coupling porewater chemistry to soil thicknesses during steady-state denudation. Earth and Planetary Science Letters 244, 444–457.
France-Lanord, C., Evans, M., Hurtrez, J., Riotte, J., 2003. Annual dissolved fluxes from Central Nepal rivers: budget of chemical erosion in the Himalayas. Comptes Rendus Geoscience 335, 1131–1140.
Gabet, E.J., 2007. A theoretical model coupling chemical weathering and physical erosion in landslide-dominated landscapes. Earth and Planetary Science Letters 264, 259–265.
Gabet, E.J., Mudd, S.M., 2009. A theoretical model coupling chemical weathering rates with denudation rates. Geology 37, 151–154.
Gabet, E.J., Burbank, D.W., Putkonen, J., Pratt-Situala, B.A., Ohja, T.P., 2004. Rainfall thresholds for landsliding in the Himalayas of Nepal. Geomorphology 63, 131–143.
Gabet, E.J., Burbank, D.W., Pratt-Situala, B., Putkonen, J., Bookhagen, B., 2008. Modern erosion rates in the High Himalayas of Nepal. Earth and Planetary Science Letters 267, 482–494.
Gaillardet, J., Dupre, B., Louvat, P., Allegre, C.J., 1999. Global silicate weathering and CO_2 consumption rates deduced from the chemistry of large rivers. Chemical Geology 159, 3–30.
Galy, A., France-Lanord, C., 1999. Weathering processes in the Ganges-Brahmaputra basin and the riverine alkalinity budget. Chemical Geology 159, 31–60.
Hamilton, J.P., Pantano, C.G., Brantley, S.L., 2000. Dissolution of albite glass and crystal. Geochimica et Cosmochimica Acta 64 (15), 2603–2615.
Hodges, K.V., Wobus, C., Ruhl, K., Schildgen, T., Whipple, K., 2004. Quaternary deformation, river steepening, and heavy precipitation at the front of the Higher Himalayan ranges. Earth and Planetary Science Letters 220, 379–389.
Hodson, A., Tranter, M., Vatne, G., 2000. Contemporary rates of chemical denudation and atmospheric CO_2 sequestration in glacier basins: an Arctic perspective. Earth Surface Processes and Landforms 25, 1447–1471.
Hren, M.T., Hilley, G.E., Chamberlain, C.P., 2007. The relationship between tectonic uplift and chemical weathering rates in the Washington Cascades: field measurements and model predictions. American Journal of Science 307, 1041–1063.
Huh, Y., Edmond, J.M., 1999. The fluvial geochemistry of the rivers of Eastern Siberia: III. Tributaries of the Lena and Anabar draining the basement terrain of the Siberian Craton and the Trans-Baikal Highlands. Geochimica et Cosmochimica Acta 63 (7/8), 967–987.
Kump, L.R., Brantley, S.L., Arthur, M.A., 2000. Chemical weathering, atmospheric CO_2, and climate. Annual Review of Earth and Planetary Sciences 28, 611–667.
Lasaga, A.C., 1998. Kinetic Theory in the Earth Sciences. Princeton University Press, New Jersey. 728 pp.
Millot, R., Gaillardet, J., Dupre, B., Allegre, C.J., 2002. The global control of silicate weathering rates and the coupling of with physical erosion: new insights from rivers of the Canadian Shield. Earth and Planetary Science Letters 196, 83–98.
Muir, I.J., Bancroft, M., Shotyk, W., Nesbitt, H.W., 1990. A SIMS and XPS study of dissolving plagioclase. Geochimica et Cosmochimica Acta 54, 2247–2256.
Oliva, P., Viers, J., Dupre, B., 2003. Chemical weathering in granitic environments. Chemical Geology 202, 225–256.
Pratt-Sitaula, B.A., Garde, M., Burbank, D.W., Oskin, M., Heimsath, A., Gabet, E.J., 2007. Bedload-to-suspended load ratio and rapid bedrock incision from Himalayan landslide-dam lake record. Quaternary Research 68, 111–120.
Putkonen, J., 2004. Continuous snow and rain data at 500 to 4400 m altitude near Annapurna, Nepal, 1999–2001. Arctic, Antarctic and Alpine Research 36 (2), 244–248.
Raymo, M.E., Ruddiman, W.F., 1992. Tectonic forcing of late Cenozoic climate. Nature 359, 117–122.
Raymo, M.E., Ruddiman, W.F., Froelich, P.N., 1988. Influence of late Cenozoic mountain building on ocean geochemical cycles. Geology 16, 649–653.
Riebe, C.S., Kirchner, J.W., Granger, D.E., Finkel, R.C., 2001. Strong tectonic and weak climatic control of long-term chemical weathering rates. Geology 29 (6), 511–514.
Riebe, C.S., Kirchner, J.W., Finkel, R.C., 2004. Erosional and climatic effects on long-term chemical weathering rates in granitic landscapes spanning diverse climate regimes. Earth and Planetary Science Letters 224, 547–562.
Searle, M.P., Godin, L., 2003. The south Tibetan detachment and the Manaslu leucogranite: A structural reinterpretation and restoration of the Annapurna–Manaslu Himalaya, Nepal. Journal of Geology 111, 505–523.
Stallard, R.F., Edmond, J.M., 1983. Geochemistry of the Amazon 2. The influence of geology and weathering environment on the dissolved load. Journal of Geophysical Research 88 (C14), 9671–9688.
Tipper, E.T., Bickle, M.J., Galy, A., West, A.J., Pomies, C., Chapman, H.J., 2006. The short term climatic sensitivity of carbonate and silicate weathering fluxes: insight from seasonal variations in water chemistry. Geochimica et Cosmochimica Acta 70, 2737–2754.
Urey, H.C., 1952. The planets: their origin and development. Yale University Press, York, Pa. 245 pp.
Waldbauer, J.R., Chamberlain, C.P., 2005. Influence of uplift, weathering and base cation supply on past and future CO_2 levels. In: Ehrlinger, J.R., Cerling, T.E., Dearing, M.D. (Eds.), A History of Atmospheric CO_2 and Its Effects on Plants, Animals, and Ecosystems. : Ecological Studies. Springer Verlag, Berlin, pp. 166–184.
Walker, J.C.G., Hays, P.B., Kasting, J.F., 1981. A negative feedback mechanism for the long-term stabilization of Earth's surface temperature. Journal of Geophysical Research 86, 9776–9782.
West, A.J., Bickle, M.J., Collins, R., Brasington, J., 2002. Small-catchment perspective on Himalayan weathering fluxes. Geology 30 (4), 355–358.
West, A.J., Galy, A., Bickle, M.J., 2005. Tectonic and climatic controls on silicate weathering. Earth and Planetary Science Letters 235 (1–2), 211–228.
White, A.F., Blum, A.E., 1995. Effects of climate on chemical weathering in watersheds. Geochimica et Cosmochimica Acta 59 (9), 1729–1747.
White, A.F., Blum, A.E., Bullen, T.D., Vivit, D.V., Schulz, M.S., Fitzpatrick, J., 1999. The effect of temperature on experimental and natural chemical weathering rates of granitoid rocks. Geochimica et Cosmochimica Acta 63 (19/20), 3277–3291.
Wobus, C., Hodges, K.V., Whipple, K., 2003. Has focused denudation sustained active thrusting at the Himalayan topographic front? Geology 31 (10), 861–864.
Wolff-Boenisch, D., Gabet, E.J., Burbank, D.W., Langner, H., Putkonen, J., 2009. Spatial variations in chemical weathering and CO_2 consumption in Nepalese High Himalayan catchments during the monsoon season. Geochimica et Cosmochimica Acta 73, 3148–3170.